Atmosphere, 20(2), 211-219 June 2010

Ocean Dynamic Processes Responsible for the Interannual Variability of the Tropical Indian Ocean SST Associated with ENSO

Jong-Seong Kug[1,*] and Soon-Il An[2]

Korea Ocean Research and Development Institute Department of Atmospheric Sciences, Yonsei University

(Manuscript received 5 April 2010; in final form 26 May 2010)

Abstract

The interannual variability of the tropical Indian Ocean SST is investigated by analyzing the ocean assimilation data. It is significant that since 1970, ENSO events frequently followed the Indian Ocean Dipole event. The SST tendency due to the dynamical SST advections over the tropical Indian Ocean sufficiently overwhelms that due to other thermodynamic process during the fall and winter of ENSO. Especially, the strong cooling due to the anomalous vertical advection by the mean upwelling and the warming due to the horizontal advection are attributed to the cold SST during the fall and the warm SST during the winter, respectively. The significant warming between winter and spring over the southwestern Indian Ocean turns out to be due to the vertical advection of the mean subsurface temperature by the anomalous upwelling during the winter and the vertical advection of the anomalous subsurface temperature by the mean upwelling from winter to spring. We speculate that when the Indian Ocean Dipole events concurred with the ENSO, the surface wind is so strong enough as to generate the change in the SST dynamically and overwhelm the SST changes associated with other effects.

Key words: ENSO, Indian Ocean Dipole, Ocean Dynamical Process

1. Introduction

In 1997 fall, during the one of the strongest El Nino events of the century, strong cooling in the eastern Indian Ocean has been concurred (Webster *et al*. 1999; Ueda and Matsumoto, 2000). In fact, a number of similar cooling in the eastern Indian Ocean and concurrent warming in the western Indian Ocean especially during fall, which is sometimes referred to 'Indian Ocean Dipole mode' (Saji *et al*. 1999), was recorded during the past 50 years that are either related to ENSO mostly or not related to ENSO. On one hand, thus it is natural to suppose the El Nino can influence the SST variability of the Indian Ocean in a way of an atmospheric bridge. On the other hand, however, it is also expectable that the local air-sea interaction possibly generates them. Thus, the interannual variation over the Indian Ocean during the developing phase of ENSO might be either externally forced by ENSO or internally generated by the local atmosphere-ocean interaction. In this sense, it is hard to separate from one excited locally to the other forced externally.

The relationship between ENSO and Indian Ocean Dipole event reflected on the statistical speculation clearly shows interdecadal variations (Ashok *et al*. 2001; An 2004). Thus, decade-to-decade investigation is inevitable. Fortunately, since 1970 that exactly overlaps our investigation period, most of the Indian Ocean Dipole events concurred with the ENSO (the correlation coefficient between the winter mean Nino-3 index and the fall mean Indian Ocean Dipole index defined by Saji *et al*. (1999) for 1970 ~ 1998 is 0.78). Thus, our speculation here based on the ENSO index will be applicable for either ENSO case or the Indian Ocean Dipole case. Besides the surface wind and SST anomaly patterns for the Indian Ocean Dipole mode events are similar to those associated with ENSO during the past several decades, meaning that the our speculation can even apply the cases

*Corresponding Author: Dr. Jong-Seong Kug, Korea Ocean Research and Development Institute, Ansan, 425-600, Korea.
Phone: +82-31-400-7749, fax: +82-31-408-5820
E-mail: jskug@kordi.re.kr

for other decades.

During the El Nino (La Nina) anomalous solar radiation over the eastern Indian Ocean increases (decrease) due to the suppressed (enhanced) so less cloudness (Klein *et al*. 1999; Venzke *et al*. 2000), and thus it causes the warming (cooling) of the surface. However, during the fall of El Nino the SST anomaly in that region becomes negative (positive). Causes that possibly bring this excessive cooling may be the intensified coastal upwelling by the anomalous southeasterly wind and the enhancement of the latent heat loses due to the larger wind speed. So far, it is unclear which process is more effective, and also other unknown dynamical process is needed to be explored. In addition, the change in solar radiation over the western Indian Ocean is too weak to cause the sustained warming (cooling) over the southeastern Indian Ocean during El Nino (La Nina). Ueda and Matsumoto (2000) and Xie *et al*. (2002) suggested that strong easterlies had the warm SST accumulated in the eastern Indian Ocean transport up to the western Indian Ocean, which in turn induces the SST change in that region. During the El Nino (La Nina), there is the easterly (westerly) anomaly along the equator and the southeasterly (northwesterly) anomaly along the eastern coastal area and its extension near Sumatra and Java, which bring the change in the oceanic circulations and finally the change in SST. Although several mechanism have been suggested, the detail analysis based on the SST budget, which may improve our understanding on the SST changing mechanism, is not investigated yet.

In this paper, we choose the ENSO index as the reference time series. It presumably brings the result to be skewed to the ENSO related signal, but this skewness might be negligible because of again the high correlation between ENSO and Dipole mode events. Based on the ENSO index, we investigate how the dynamical response to the ENSO-related wind stress anomalies can generate the SST anomaly over the tropical Indian Ocean. Specifically, in the section 2 we introduce the data and analysis method, and in the section 3 show the atmosphere and ocean patterns associated with El Nino. In the section 4, by evaluating the SST advection terms, the mechanism related to the SST variation due to the dynamic process with the emphasis of fall season is explored. Summary and discussion is added in the section 5.

2. Data and Analysis method

The data utilized are the monthly means of Simple Ocean Data Assimilation (SODA) product. The data period is the 30 years from 1970 to 1999, a period when the use of expendable bathythermograph (XBT) and conductivity-temperature-depth (CTD) sensors became widespread worldwide, resulting in a great increase in the number of measurements below 200m (Carton *et al*. 2000a,b). Xie *et al*. (2002) shows that the SODA data has a good agreement with XBT observation in their Indian Ocean analysis. It is available at 1X1 resolution in the mid-latitudes and 1X0.45 longitude-latitude resolution in tropics, and has 20 vertical levels with 15m resolutions near the sea surface. The variables used are the zonal, meridional and the ocean temperature at each layer from the surface (7.5m) to 52.5m depth. In the present study, well-mixed layer depth is fixed at 45m depth which includes 3 vertical layers.

In this study, the evolutionary feature of the Indian Ocean dynamic process is described by the lag-linear-regressions with the NINO3.4 SST during the ENSO mature season (Nov.-Jan). Noted that all analyses are stratified by calendar month because the Indian Ocean variability is strongly phase-locked to the seasonal cycle (Xie *et al*. 2002).

3. Impact of ENSO on the tropical Indian Ocean

3.1 Surface wind and SST

The warm (cold) SSTA over the central and eastern Pacific occurring during El Nino (La Nina), caused for the major convection center in the tropics to move to the central Pacific, and in turn the anomalous vertical motion in the maritime continent is suppressed. Due to this suppression, the anomalous easterly can be expected. Figure 1 shows linear regression of SST and wind stress with respect to the NINO3.4 SST. During SON and the DJF, mature phase of El Nino, the anomalous easterly

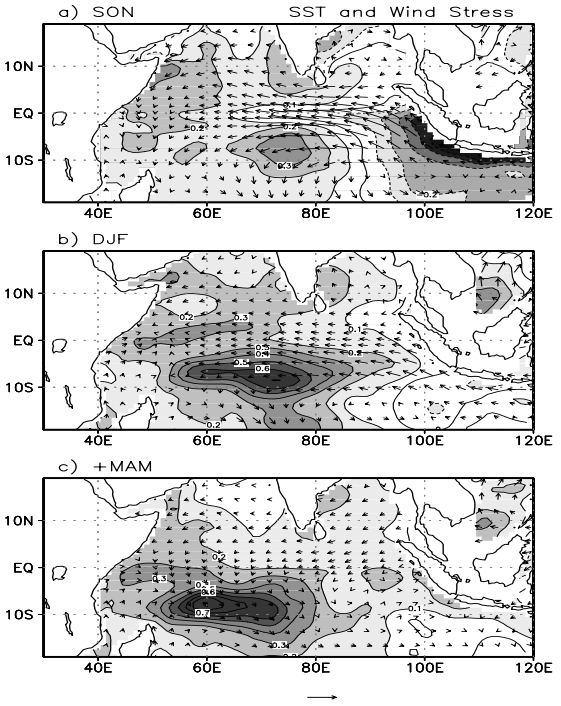

Fig. 1. Linear regression of SST (contour) and wind stress (vector) with respect to NINO3.4 SST during a) SON(0), b) D(0)JF(1) and c) MAM(1).

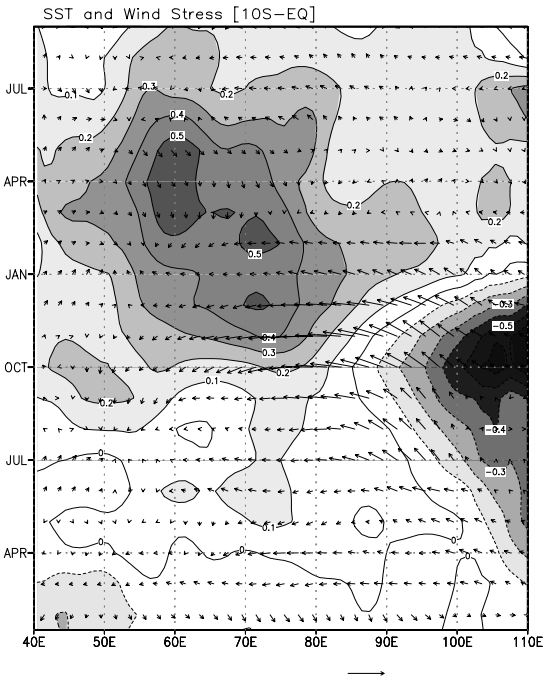

Fig. 2. Hovmuler diagram of the linear regression of SST (contour) and wind stress (vector) averaged over 10S ~ EQ with respect to NINO3.4 SST.

over the equatorial Indian Ocean and the southeasterly over the southeastern Indian Ocean are dominant. In the decaying phase of El Nino (Fig. 1c), the wind over the whole Indian Ocean becomes weaker (Fig. 1c). Note that the strong easterly anomaly during the fall season, may be related to an addition intensification due to the local air-sea interaction process representing the strong east-west SST contrast (Fig. 1a) (Saji *et al*. 1999; Webster *et al*. 1999). This east-west SST contrast disappears during the El Nino mature phase (Fig. 1b) and is even much weaker during after the El Nino mature phase (Fig. 1c). Over the southern Indian Ocean, warm SST is appeared during SON, and it gradually develops and slowly propagates to the west.

The zonal evolution of SST and surface wind over the tropical Indian Ocean (10S-EQ) is much clearly shown in the Fig. 2. The easterly anomaly starts to blow on March and the negative SSTA in the eastern Indian Ocean appear as well. The SST in the eastern Indian Ocean gradually becomes colder and expands to the west until October and after then rapidly weaker and shrinks toward the coastal region and totally gone on January. On the other hand, the warm SST anomaly prominently develops since September and it is maximized during December ~ May. It tends to propagate to the west (Xie *et al*. 2002). SST anomaly over the whole Indian Ocean becomes very small after September. Note that the maximum cold SST anomaly over the eastern Indian Ocean leads the maximum warm SST anomaly over the western Indian Ocean by about 4-month. The maximum wind occurs during Oct ~ Dec.

3.2 Ocean dynamic fields

Figure 3 shows the surface layer current defined as a vertically averaged value from the surface to 45 m depth and upwelling at 45 m depth associated with El Nino. The strong equatorial current during SON flows toward the west, which is the same direction as the surface wind aims, meaning the wind driven surface current. Associated with this current, the equatorial upwelling over the

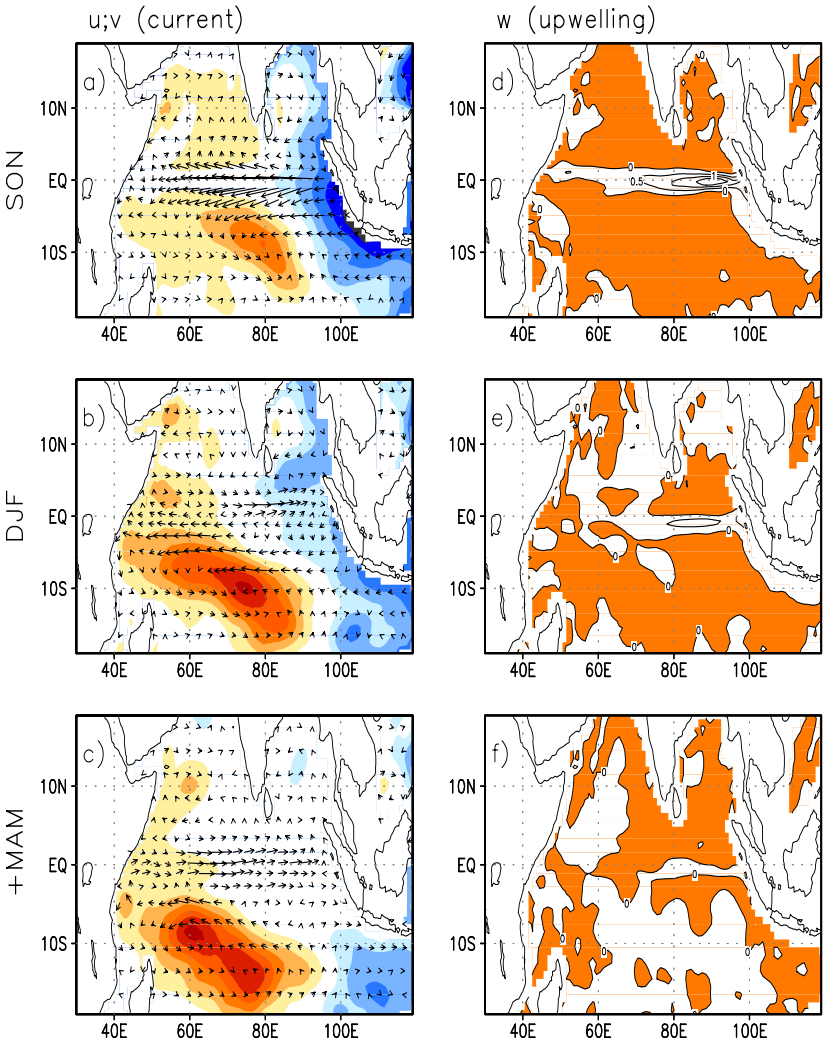

Fig. 3. The same as Fig. 1 except for ocean mixed layer current (vector, left panal), 20C isothermal depth (shaded, left panal), and upwelling (right panel).

eastern Indian Ocean is dominant. Equatorial surface easterly wind stress generates equatorial upwelling by the Ekman transport. During DJF, the equatorial current becomes weaker and the upwelling as well (Fig. 3b and 3e) due to the weak surface wind . During MAM, the upwelling almost is gone and the current is reversed (Fig. 3c and 3f). This westward current is presumably the geotropic current as a result of a balance with the east-west pressure gradient. This is because the surface wind during MAM is too weak to maintain the current, while the east-west contrast of the 20C isotherm depth is big during this period (Fig. 4). Ocean dynamics fields adjust to a given surface wind stress with a lag. The lag is related to the oceanic wave speed.

A delayed response of the ocean dynamics fields to the surface wind stress is clearly shown in Fig. 4. The maximum 20C isotherm depth appears 5 months later when the surface wind is the maximum. The value shown in Fig. 4 is averaged one between 10S ~ EQ, and thus, a possible dominant wave over that latitudinal band is the Rossby wave and its phase speed is about 8 m/s. The deepening in the central Indian Ocean and the shoaling in the eastern Indian Ocean during SON is well matched to the strong easterly surface wind stress so it must be

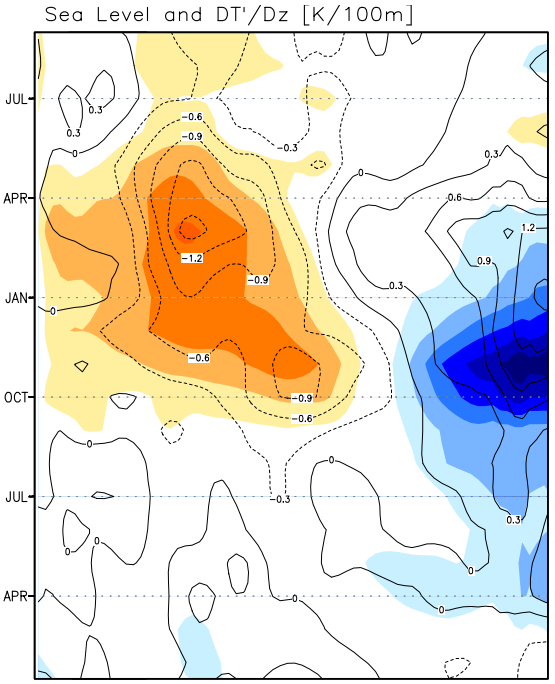

Fig. 4. Same as Fig. 2 except for 20C isothermal depth (contour) and vertical temperature gradient (shaded).

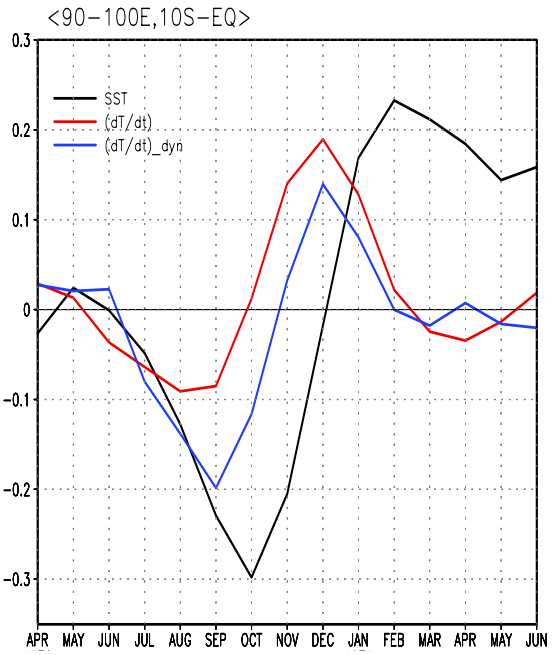

Fig. 5. Linear regression of SST (black line), SST tendency (red line), and sum dynamical advection terms (blue) averaged over 90-100E, 10S-Eq with respect to NINO3.4 SST. Sum of dynamical adevection terms are calculated based on Eq. (1).

a directly wind driven. The strong downwelling signal in the western Indian Ocean during March is originated from the central Indian Ocean during September, but it seems to be influenced by local air-sea interaction too because the amplitude has been increased during the propagation. However, both the deep thermocline depth in the western Indian Ocean and the shallow thermocline depth in the eastern Indian Ocean quickly return to back the normal state since Jun. Thus, one may expect that since Jun, the dynamical process doest not play a role to change the Indian Ocean SST any more.

4. Evolution of SST advection terms associated with ENSO

As shown below in Eq. (1), the SST anomaly is governed by the three-dimensional advection terms and the heat flux at the ocean surface. In the present section, we estimate the contribution of each advection term to the SST tendency using the SODA data.

$$\frac{\partial T'}{\partial t} = -u_M \frac{\partial T'}{\partial x} - u' \frac{\partial T}{\partial x} - v_M \frac{\partial T'}{\partial y} - v' \frac{\partial T}{\partial y} - (w_M + w') \frac{\partial T'}{\partial z} - w' \frac{\partial T_M}{\partial z} - Q' \quad (1)$$

where T' is the SST anomaly, u' and v' are the anomalous zonal and meridional currents, respectively, and w' the anomalous upwelling velocity. Note that the above equation is not the same as that used for the assimilation system. However, the aim of the present study is not to estimate the exact budget of the SST anomaly but to evaluate the relative importance of the advective terms in the SST equation. Other residual terms (e.g., the diffusion and vertical mixing terms, and etc) not expressed in the above equation can be included in Q'. Note that among the dynamical advective process, the diffusion by eddy, and eddy heat flux are not accounted here. Besides the monthly mean data used, and thus the advection by the high frequency wave is also not included.

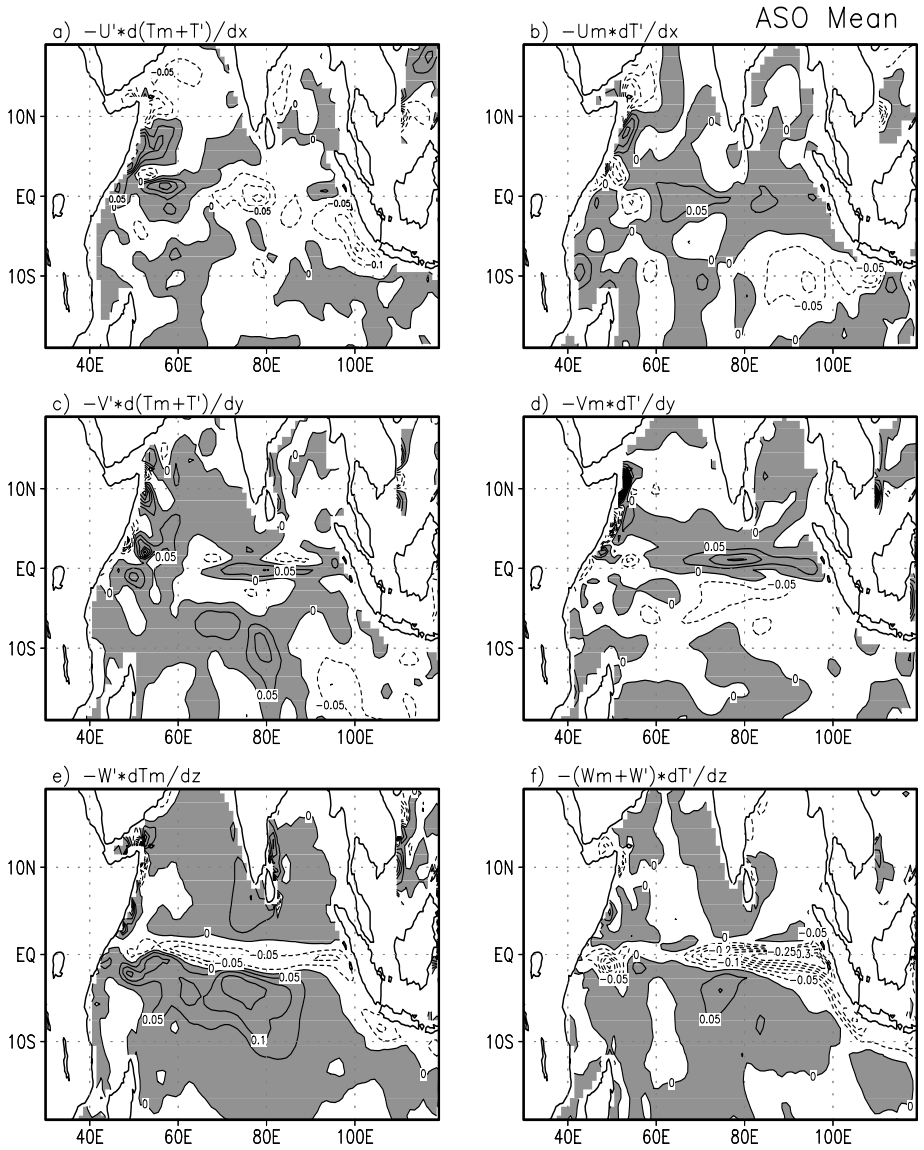

Fig. 6. Linear Regression of each term from Equation (1) during ASO with respect to NINO3.4 SST. Positive value is shaded.

As mentioned in the introduction, our focus is the mechanism of the SST change through the dynamical process. It has been argued that the thermodynamic process such as the surface heat flux plays a major role of changing of SST. However, the evolution of the SST tendency due to the dynamical process resembles to that of total SST tendency. For instance, SST change in the eastern Indian Ocean (90-100E, 10S-EQ) during El Nino is adequately explained by the SST tendency due to the dynamical process only (Fig. 5). The residual (indicating Q in Eq. (1)), which mostly is attributed to the solar radiation and the latent heat flux, increases from zero to 0.12 C/month until October, after then decrease, indicating that the latent heat loss is not enough to overcompensate the increase of the Solar Radiation. This is also happened during 1997-98 El Nino (Murtugudde *et al*. 2000). Murtugudde *et al*. (2000) showed that the phase change over the eastern Indian Ocean from the cooling during

fall to the warming during the winter is mainly due to the net heat flux, while in our calculations, the Q quickly decreases during winter and the warming tendency due to the dynamical advections increases.

Figure 6 shows the linear regression of the temperature advection terms in the right-hand side of Eq. (1) during ASO with respect to the NINO3.4 SST. The mean temperature advection by anomalous zonal current, $-u'\partial T_m/\partial x$ plays a role of cooling over the equatorial central and south far eastern Indian Ocean (Fig. 6a). The cold advection in the equatorial central Indian Ocean might be attributed to the nonlinear zonal advection term, $-u'\partial T'/\partial x$, resulting from the strong westward current anomaly and the anomalous negative zonal SST gradient (the zonal gradient of the mean SST is relatively weak.). Another important role of this term is the zonal expansion of the cold water, which has been generated along the coastal area of Sumatra and Java. Two prominent cold advections are completely disappeared since DJF (not shown). The anomalous temperature advection by mean zonal current ($-u_m\partial T'/\partial x$) is positive over the whole tropical Indian Ocean (5S-5N) (Fig. 6b). This is because the equatorial westerly jet, so called 'Wyrtki Jet' (Wyrtki 1973) during the boreal fall and spring becomes its maximum and the zonal contrast of SSTA as well. However, this term is weak during March ~ May (MAM) because of a weak zonal SST gradient (not shown).

The mean temperature advection by anomalous meridional current, $-v'\partial T_m/\partial y$ is not significant over all (Fig. 6c). While during DJF, there is a warming tendency by this term over the equatorial Indian Ocean (not shown). On the other hand, the anomalous temperature advection by mean meridional current ($-v_m\partial T'/\partial y$) clearly shows a warming tendency over the equatorial Indian Ocean, especially central region (Fig. 6d), because of the convergence of the mean meridional current into the equator and the cold SST anomaly over the equatorial region.

Figure 6e shows the SST tendency due to the mean thermal advection by the anomalous upwelling ($-\{\mathbf{M}(W_m+W')-\mathbf{M}(W_m)\}dT_m/dz$). The warming tendency due to this term is dominant between 10S and Equator, possibly due to the anomalous downwelling by the convergence of the Ekman current. The equatorial upwelling over the western Indian Ocean contributes the cooling over the very confined area. The equatorial cooling becomes much stronger by the anomalous thermal advection by the mean upwelling ($-\mathbf{M}(W_m)\,d(T_m+T')/dz$), which appears over the whole equatorial Indian Ocean, especially in the central-to-eastern region (Fig. 6f). Note that although the data is not enough to resolve the coastal area, but the strong cooling along the coastal zone near Sumatra and Java islands is significantly shown in Fig. 6f. Note also that the warming tendency over the south-central Indian Ocean, which may be due to the anomalous subsurface temperature change (dT'/dz) as shown in Fig. 4.

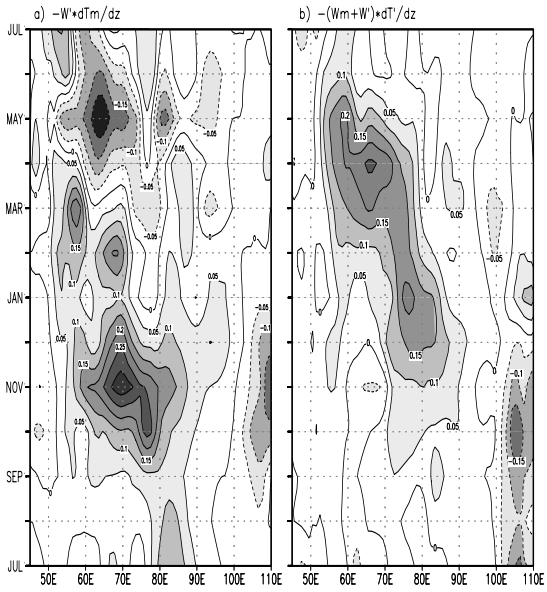

Fig. 7. Same as Fig. 2 except two vertical advection terms from Equation (1).

In the off equatorial region, the wind stress curl associated with the equatorial easterlies induces anomalous Ekman convergence (downwelling), forcing a pair of downwelling equatorial-trapped Rossby waves that slowly propagates to west. Fig. 7 clearly shows that the warming tendency propagates to the west accompanied with the Rossby wave propagation over the tropical southern Indian Ocean. During the fall, the warming tendency by ($-\{\mathbf{M}(W_m+W')-\mathbf{M}(W_m)\}dT_m/dz$) is much bigger than that by ($-\mathbf{M}(W_m)d(T_m+T')/dz$). This is

because the anomalous upwelling driven by the wind stress is dominant. However, as the wind stress becomes weaker, the SST tendency by $(-\{\mathbf{M}(W_m+W')-\mathbf{M}(W_m)\}\, dT_m/dz)$ is smaller, and than disappears since March. On the other hand, the warming by $(-\mathbf{M}(W_m)d(T_m+T')/dz)$ continues until May. It has been argued that the slowly propagating downwelling Rossby waves generated by the easterlies with a slight time lag change the sub-s urface temperature over the southern Indian Ocean until MAM (Murtugudde *et al*. 2000; Xie *et al*. 2002).

5. Concluding Remarks

Using ocean assimilation data, the dynamical processes that attribute the interannual change of the Indian Ocean SST are investigated. The SST tendency due to the dynamical SST advections over the tropical Indian Ocean sufficiently overwhelms that due to other thermodynamic process during the fall and winter of ENSO. Especially, the strong cooling due to the anomalous vertical advection by the mean upwelling and the warming due to the horizontal advection are attributed to the cold SST during the fall and the warm SST during the winter, respectively. The significant warming between winter and spring over the southwestern Indian Ocean turns out to be due to the vertical advection of the mean subsurface temperature by the anomalous upwelling during the winter and the vertical advection of the anomalous subsurface temperature by the mean upwelling from winter to spring. We speculate that when the Indian Ocean Dipole events concurred with the ENSO, the surface wind is so strong enough as to generate the change in the SST dynamically and overwhelm the SST changes associated with other effects

Because our investigation focuses on the change of the Indian Ocean SST associated with the ENSO, apparently the angle of our investigating scope is restricted to be narrow down to the ENSO. However, since 1970, the El Nino (La Nina) that used to be peak during winter very frequently follows the Indian Ocean Dipole events, which is maximized during the fall. In addition, evidently, the correlation between the ENSO and the Indian Ocean Dipole events becomes higher than that during any other decades recorded instrumentally. It implies that when the Indian Ocean Dipole events concurred with ENSO, the changes in the atmosphere and ocean over the Indian Ocean are generated by the external forcing by ENSO and the internal air-sea interaction. Thus, our investigation on the SST budget can be also applied to the Indian Ocean dipole.

Acknowledgement

This work is funded by Korea Meteorological Administration Research and Development Program under grant RACS_ 2010-2007.

REFERENCES

An, Soon-Il, 2004: A dynamic link between the basin-scale and zonal modes in the tropical Indian Ocean ,Theor. Appl. Climatol., 78, 203-215.

Ashok, K., Guan, Z. and Yamagata, T. (2001). Impact of the Indian Ocean Dipole on the Relationship between the Indian Monsoon Rainfall and ENSO. *Geophys. Res. Lett.,* 28(23): doi: 10.1029/2001GL013294.

Carton, J. A., G. Chepurin, , X. Cao, and B. Giese, 2000a: A Simple Ocean Data Assimilation Analysis of the Global Upper Ocean 1950–95. Part I: Methodology. *J. Phy. Ocean.,* **30**, 294–309.

_____, _____, and _____2000b: A Simple Ocean Data Assimilation Analysis of the Global Upper Ocean 1950–95. Part II: Results. *J. Phy. Ocean.,* **30**, 311–326.

Klein, S., B. J. Soden, and N.-C. Lau, 1999: Remote sea surface temperature variations during ENSO: Evidence for a tropical atmospheric bridge. J. Climate, 12, 917-932.

Murtugudde, R., J. P. McCreary Jr., and A. J. Busalacchi, 2000: Oceanic processes associated with anomalous events in the Indian Ocean with relevance to 1997-1998. J. Geophy. Res., 105, 3295-3306.

Saji, N. H., B. N. Goswami, P. N. Vinayachandran, and T. Yamagata, 1999: A dipole mode in the tropical Indian Ocean. *Nature*, **401**, 360-363.

Sprintall, J., A. Gordon. R. Murtugudde, and D. Susanto, 2000: An Indian Ocean Kevin wave observed in the Indonesian seas during May 1997. *J. Geophys. Res*., **105**, 17,217-17,230.

Ueda, H. and J. Matsumoto, 2000: A possible triggering process of East-West asymmetric anomalies over the Indian Ocean in relation to 1997/98 El Nino. *J. Met. Soc. of Japan*, **78**, 803-818.

Webster, P. J., A. M. Moore, J. P. Loschnigg, and R. R. Leben,

1999: Coupled ocean-atmosphere dynamics in the Indian Ocean during 1997-98. *Nature*, **401**, 356-360.

Venzke, S., M. Latif, and A. Villwock, 2000: The coupled GCM ECHO-2. Part II: Indian Ocean response to ENSO. *J. Climate*, **13**, 1371-1383.

Wyrtki, K., 1973: An equatorial jet in the Indian Ocean. *Science,* **181,** 262–264.

Xie, S.-P., H. Annamalai, F. A. Schott, and J. P. McCreary, 2002: Structure and mechanisms of South Indian Ocean climate variability. *J. Climate*, **15**, 864–878.

Yu, L., and M. M. Rienecker, 1999: Mechanisms for the Indian Ocean warming during the 1997-98 El Nino. *Geophys. Res. Lett.*, 26, 735-738.